STM JOURNALS

Journal of
Water Pollution &
Purification Research

ISSN: 2394-7306
Volume 12, Issue 3, 2025
September–December
DOI (Journal): 10.37591/JoWPPR

https://journals.stmjournals.com/jowppr

Research JoWPPR

Synthesis of Activated Carbon from Corn Cob and Factors Affecting its Adsorption and Desorption Efficiency of Cationic Brilliant Green Dye

Mizbawu Kanea Gurmu[1], V. Murali M.E.[2], Tariku Tadesse Gemeda[1], Yoobsan Ejeta Amensisa[3,*]

Abstract

Extreme dye pollutants released from textile, leather, and pulp industries are becoming a major concern for water. These pollutants are highly toxic to living things. The major objective of this study was to prepare low-cost and efficient activated carbon from corncob (CCAC) adsorbent through the H_2SO_4 activation method and characterize its suitability for removing brilliant green dye (BGD) from aqueous solution. The adsorption and desorption efficiency of the prepared CCAC sample were evaluated. The CCAC samples were found to be amorphous materials based on XRD measurements. According to the FTIR spectrum, the CCAC's chemical structure included a variety of functional groups. The morphology of CCAC was studied using the SEM image analysis. This study investigated the factors affecting the adsorption and desorption efficiency of the synthesized CCAC. As a result, the maximum adsorption efficiency of 95.7, 94.37, 98.1, and 99.56% were achieved at pH=8, contact time =20 min, the dosage of CCAC=0.3 g, and initial concentration =43 mg/l, respectively. The BGD removal fits into the Freundlich isotherm model, which is different from the Langmuir model, with a correlation coefficient R^2 of 0.999. Batch experiments were performed on synthetic wastewater and the effect of operating parameters such as pH, initial concentration of dye, contact time, and adsorbent dosage were studied. The adsorption mechanism fits more Freundlich isotherm than with the correlation coefficient R^2=0.999. According to the investigation, a maximum adsorption capacity of 98.4 mg/g was achieved. The maximum and minimum desorption efficiency of 92.45 and 43.8% were obtained at 1 M HCl and 0.125 M CH_3OH, respectively. In general, the synthesized CCAC was effectively used to remove BGD from aqueous solution with desired efficiency and therefore, it can be a promising material for the removal of dye pollutants from water and wastewater.

***Author for Correspondence**
Yoobsan Ejeta Amensisa
E-mail: yobsan.ejeta@obu.edu.et

[1]Lecturer, Department of Environmental Engineering, College of Engineering and Technology, Bule Hora University, Bule Hora, Ethiopia
[2]Former Lecturer, Department of Environmental Engineering, College of Engineering and Technology, Bule Hora University, Bule Hora, Ethiopia
[3]Lecturer, Department of Food Technology and Process Engineering, Oda Bultum University, Chiro, Ethiopia

Received Date: April 08, 2025
Accepted Date: June 06, 2025
Published Date: June 10, 2025

Citation: Mizbawu Kanea Gurmu, V. Murali M.E., Tariku Tadesse Gemeda, Yoobsan Ejeta Amensisa. Synthesis of Activated Carbon from Corn Cob and Factors Affecting its Adsorption and Desorption Efficiency of Cationic Brilliant Green Dye. Journal of Water Pollution & Purification Research. 2025; 12(3): 27–44p.

Keywords: Adsorption, brilliant green dye, corn cob, activated carbon, desorption

INTRODUCTION

Nowadays, huge amounts of effluents released from the manufacturing industries and direct contact with surface water have been highly affecting its quality and becoming a major concern [1]. The pollutants discharged from industries naturally consist of different toxic compounds that contaminate water [2]. Serious environmental issues are caused by the discharge of dyes into water and wastewater from the textile, cosmetic, paper, coloring industries, etc. [3] Water bodies with colored surfaces have improper solar penetration,

slower photosynthesis, stunted growth of aquatic life, and altered gas solubility [4]. The pulp paper and dying industries make extensive use of brilliant green dye (BGD), a cationic dye derived from diamino-triphenylmethane. The molecular structure of BDG is shown in Figure 1. Due to its high solubility (100 g/l), brilliant green dye is a commonly used dye. On the other hand, because of its high volatility and cationic nature, brilliant green dye pollutes the atmosphere. According to reports, BGD has been linked to a number of health issues, including irritation of the skin and respiratory tract, coughing, dyspnea, and gastrointestinal system irritation, which manifests as nausea, diarrhea, and stomach pain [5]. Hence, the elimination of BGD from the effluents before discharging into the environment is mandatory [5].

The investigations have documented methods for removing colors from water and wastewater using physical, chemical, and biological methods. The physicochemical adsorption method was an appropriate technique with suitable adsorbents for effectively removing BDG at the desired efficiency due to its many advantages over other methods [6]. The physiochemical adsorption method has several advantages, including insensitivity to harmful compounds, ease of operation, and simplicity of design. Agricultural waste materials were used as a sustainable and low-cost source of adsorbent extraction [7]. Corncob is a lignocellulosic material left as a byproduct in a maize preparation factory. Activated carbon was prepared using this agricultural residue as a source. It was reported that activated carbon was an efficient adsorbent for BDG removal [8, 9]. The remarkable adsorption effectiveness of activated carbon (powdered or granular) for organic molecules even from dilute solutions gives the adsorption process an edge over the other methods. Because of its sufficient surface area and adsorption capacity, commercial activated carbon is an effective adsorbent for eliminating dyes; yet, it is still costly. Thus, researches are looking for alternative inexpensive adsorbent material for the removal of organic contaminants [10, 11].

Different biomass and agricultural byproducts including wood, coal, peat, nutshells, sawdust, bones, husk, and so on were used as sources for the preparation of activated carbon [12–15]. However, there has not been much discussion of using corncob-derived activated carbon as an adsorbent to remove BGD from an aqueous solution. Thus, the objective of this work was to prepare the activated carbon from corncob and examine its adsorption and desorption efficiency in removing cationic BDG from an aqueous solution. Fourier transform infrared spectroscopy, XRD, and UV-vis spectroscopy were used to characterize the produced activated carbon. Some relevant factors like pH of the solution, initial BGD concentration, adsorbent dosage, and contact time on activated carbon adsorption efficiency were systematically studied.

MATERIALS AND METHODS

Raw Materials and Chemicals

The raw materials used for the experiments are corncobs that were collected from local farmers of Bule Hora, West Guji, Oromia, Ethiopia.

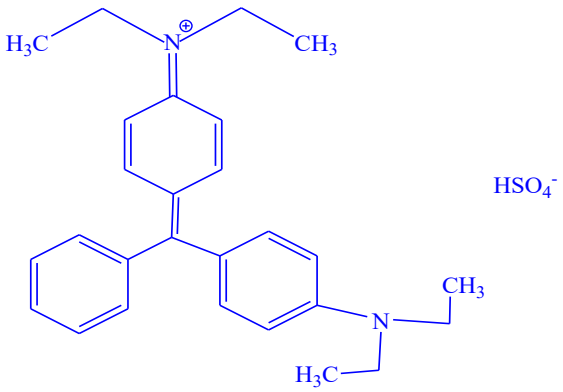

Figure 1. Molecular structure of BGD.

The study experiments were conducted at the Laboratory of Chemical Engineering, and Chemistry Department at Bule Hora University, Ethiopia. All chemicals used were of analytical grade. The apparatus used were a ceramic crucible, conical flasks, measuring cylinders, funnel, ceramic crucible, beakers, Whatman filter paper, hot plate, blast drying oven (DHG-9055A), box-type resistance furnace (SX-2.5-12), refrigerator, fume hood (SW-TFG-12), knife, mortar and pestle (grinder), shaker and beaker, an electronic balance (AS220-R2), and pH meter (pH-016). The chemicals, reagents, and materials required for the laboratory works were H_2SO_4 (98%, Newdehli-11002 India), $NaHCO_3$ (99%Maharashtra, India), brilliant green powder ($C_{27}H_{34}N_2O_4S$, AR 85 Merck, Bangalore, India), NaCl (99.5) (LOBA Chemie, India), HCl (AR 35, Sigma-Aldrich, Bangalore, India), NaOH (98%, NN36HY, UK) and distilled water. X-ray diffraction (XRD-700), Fourier transform infrared (FTIR), scanning electron microscopy (SEM), and a UV-visible double beam spectrophotometer (UV-5000) were the instruments utilized for the characterization.

Sample Preparation and Experimental Procedures

The sample preparation and experimental methodology is shown in Figure 2.

Synthesis of Corn cobs activated carbon

Initially, collected corncobs were washed several times using distilled water followed by sun-drying for about 48 h, and inserted into the oven at 105ºC to remove any moisture content from the surface [16]. The dried corncobs were then divided into various pieces, including longitudinal pieces. Afterward, the activation process was done with H_2SO_4 following the procedures reported by Kolur *et al*. [17]. Then, 100 g of grounded corncobs were weighed into a clean, dry beaker containing 200 ml of H_2SO_4 for about 24 h, which was then refluxed in a fume hood for 4 h. The paste obtained was then filtered, and the solid phase left on the filter was then dried in an oven at 105°C for 24 h. Then, dried small pieces of CC were put into a furnace to heat at a temperature of 450°C to produce charcoal. The obtained charcoal product was then cooled, filtered, and then washed in 1% $NaHCO_3$ solution to remove any residual acidic impurities. After that, the beaker was covered and remained at room temperature for 24 h. Next, the product was washed with distilled water until its pH became 6.5. Finally, the as-prepared corncob-activated carbon (CCAC) sample was dried in an oven overnight at a temperature of 105ºC, then, sieved to 1–2 mm and kept in a glass bottle for the forthcoming experiments.

Characterization of the Synthesized Adsorbents

Fourier Transform Infrared (FTIR) Analysis

Through the use of FTIR, the surface functional groups of the activated carbon were identified in this investigation. The 4000–500 cm^{-1} range was used to record the spectra.

X-ray Diffraction (XRD)

An XRD diffraction analysis was performed to determine the crystallinity of the CCAC. The X-ray diffraction (XRD-700) was performed on Cu Kα radiation (k=0.1540 nm) and 2θ ranging from 5 to 70º.

Scanning Electron Microscopy (SEM)

Surface morphology has a characteristic role in determining the surface area adsorption. It was reported that a high surface area increases the contact efficiency between dyes to be removed [18]. In this work, the surface morphology of CCAC was investigated using scanning electron microscopy (SEM).

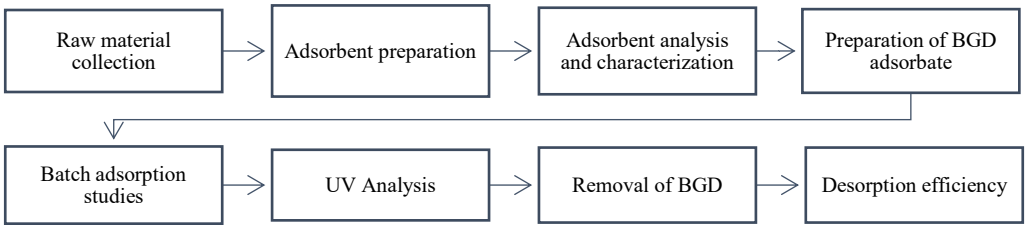

Figure 2. Flow scheme of methodology.

Point of Zero Charge Analysis

It was reported that when the pH of the solution exceeds the point zero charge, BGD adsorption could be enhanced. The pH of point zero charges (pHpzc) findings of the CCAC adsorbent were ranged between 2 and 12. Below pHpzc the value, the surface of the adsorbent is positively charged due to protonation, encouraging anion adsorption. The surface of the CCAC contains a negative charge above the pHpzc, which inhibits anion species adsorption [19].

Preparation of BGD Adsorbate

The stock solution of 1000 ppm was prepared by dissolving an accurately weighed amount of BG dye in 1 l of distilled water. The stock solution was further diluted using a dilution equation for the experimental solution of the desired concentration using distilled water [20]. In this study, 1 g of BGD was dissolved in 1 l of distilled water to prepare 1 g/l of stock solution. A magnetic stirrer ensured the homogenization of the solution. The concentration of BGD used was from 10 to 150 mg/l. To determine the standard calibration equation, this study used five series of standard BGD solutions (10, 30, 50, 70, and 90 mg/l) which were then prepared by diluting the intermediate solution of BGD with distilled water. Working standards and blank solution were tested at a maximum wavelength of 625 nm in a UV-visible Spectrophotometer [21], and calibration curves with five points were created. Following that, direct measurements of the sample absorbance were made after the sample solutions were brought to the UV-visible spectrophotometer. Finally, the linear relationship of absorbance versus concentration was plotted using Eq. (1), and the equation for final concentrations was found from the slope of the graph [22].

$$\text{Absorbance} = \text{Slope} \times \text{Ce} - \text{Intercept} \quad (1)$$

Batch Adsorption Studies

Adsorption studies were carried out by determining the solution pH, initial dye concentration, adsorbent dosage, and contact time. Prior to the adsorption experiment, which was conducted at 25°C, the pH of the solution was changed by adding either 0.1 M NaOH or 0.1 M HCl solutions. The pH of the dye solution and the pHpzc are the important factors controlling the adsorption of dyes [14]. To do that, the flask was placed on an electric shaker running at 200 rpm until adsorption equilibrium was obtained [23]. The concentration of BGD was determined using a UV-visible double-beam spectrophotometer. The adsorption capacity of the BGD was calculated using the following expression:

$$qe\left(\frac{\text{mg}}{\text{g}}\right) = \frac{\text{C}_\text{o} - \text{C}_\text{e}}{\text{w}} \text{ V} \quad (2)$$

$$RE = \frac{\text{C}_\text{o} - \text{C}_\text{e}}{\text{C}_\text{o}} * 100 \quad (3)$$

Where; *RE*: removal efficiency, C_o (mg/l): the initial concentration of BGD, C_e (mg/l): the equilibrium liquid phase concentration of BG, *V* (l): the volume of the solution, and *m* (g) is the amount of CCAC.

Adsorption Isotherms

Langmuir Adsorption Isotherm

According to the Langmuir model, the adsorbent surface has numerous active interaction sites for the adsorption process. It is concerned with the relationship between adsorbed material and its equilibrium concentration [24]. The Langmuir adsorption isotherm model's linear form, which permits the adsorption and desorption of molecules on the surface, is explained as:

$$\frac{C_e}{Q_e} = \frac{1}{bQ_{max}} + \frac{C_e}{Q_e} \quad (4)$$

Where; Q_e *(mg/g)* denotes the mass of adsorbate adsorbed over adsorbent, C_e (mg/l), the equilibrium concentration of adsorbate acquired in the liquid phase after adsorption, Q_{max} (mg/g), the maximum adsorbate that can be adsorbed (monolayer capacity), and *b* (l/mg), the Langmuir isotherm constant.

The separation factor (R_L) factor was also calculated from the empirical constant ***b*** using the following equation given by Mansour *et al*. [21]:

$$R_L = \frac{1}{1+bC_o} \quad (5)$$

The value of R_L indicates the adsorbent's suitability for adsorption, *i.e*., the affinity between adsorbate and adsorbent. Based on the R_L factor values the adsorption can be unfavorable (R_L>1), linear (R_L=1), favorable (0<R_L<1), or irreversible (R_L=0) [25].

Freundlich Adsorption Isotherm

The Freundlich adsorption isotherm illustrates the connection between the adsorbate equilibrium concentration (Ce) in the fluid and the amount of adsorbate absorbed per unit weight of adsorbent [26]. The Freundlich model, unlike the Langmuir model, is based on multilayer adsorption and may be expressed as Eq. (6):

$$\frac{X}{M} = KC_e^{1/n} \quad (6)$$

Where; *K* and *n* are the Freundlich coefficients, *X* represents the weight of adsorbate adsorbed on *M* unit weight of adsorbent, and *Ce* is the adsorbate equilibrium concentration. Nevertheless, the equilibrium condition can also be expressed as Eq. (7):

$$Log(Q_e) = \log(k_f) + \frac{1}{n} logC_e \quad (7)$$

Where; Q_e (mg/g) is the mass of adsorbate adsorbed over adsorbent; K_f, the Freundlich capacity factor (units determined by Q_e); C_e (mg/l); is the equilibrium concentration of adsorbate in liquid phase after adsorption; and *n* is Freundlich intensity parameter. The value of the coefficients of n can be found by calculating the intercept and slope of a plot of log (Q_e) vs. log (C_e).

The value of ***n*** indicates the nature of the process, that is, if *n<1* chemical, *n=1* linear, and *n>1* is a physical process [27].

Regenerative Studies

It was reported that the reuse of adsorbents used for the removal of various types of contaminants from water and wastewater after regeneration is seen as a crucial work in circular economy goals [27]. In this study, the reuse of the adsorbents was studied as follows:

The adsorbent was first cleaned with 0.1 NaOH and then repeatedly rinsed with distilled water. Meanwhile, the regeneration of BGD is carried from a stock solution of 1000 mg/l. From this stock solution, 100 mg/l of BGD solution was prepared. Following the dilution equation, different concentrations (10, 30, 50, 70, and 90 mg/l) of solutions were prepared. Then, the effect of regeneration agents (0.125, 0.25, 0.5, and 1 M of HCl, NaCl, and Methanol, respectively), the initial concentration, and acid-to-alcohol ratios (1:0, 3:1, 1:1, 1:3, and 0:1% of HCl:1-Butanol) on regenerations of BDG were determined [28]. Lastly, a UV-visible double-beam spectrophotometer was used to assess the desorbed efficiency of BGD. In the meantime, the filtrated dye solutions were measured to calculate the adsorption efficiency of the adsorbent after undergoing the desorption process by regeneration agents. The desorption efficiency (DE) was then calculated from Eq. (8).

$$D_E = \frac{A_0 - A_d}{A_0} * 100\% \quad (8)$$

Where; D_E is desorption efficiency, and A_0 and A_d are the initial dye, and final dye concentration after adsorption, respectively.

RESULTS AND DISCUSSION

Experimental Framework for the Synthesis of Corn Cob-activated Carbon

The experimental framework for the synthesis of corn cob activated carbon is shown in Figure 3.

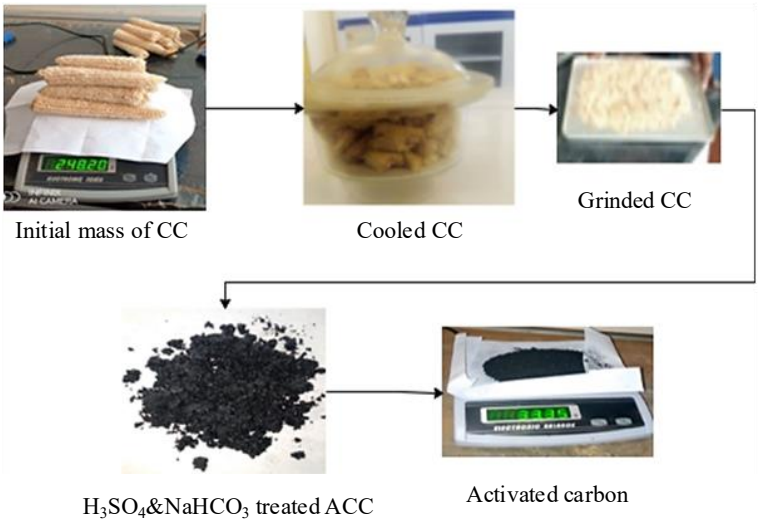

Figure 3. Photographic images of experimental workflow.

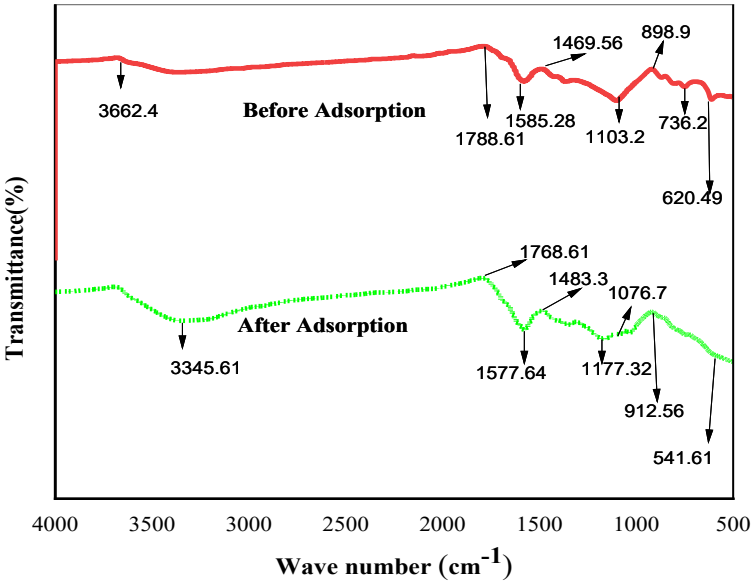

Figure 4. FT-IR spectra of synthesized CCAC before and after BGD removal.

Fourier Transform Infrared (FT-IR) analysis

The FTIR spectrum recorded for CCAC is given in Figure 4. The band gap between 3000 and 2800 cm^{-1} corresponds to the C–H vibrations in aliphatic, olefin, and aromatic hydrocarbons groups, and 1770–1650 cm^{-1} corresponds to vibration in the C=O bond [18, 29]. Similarly, the bands at 1700–1600, 1480–1420, 1430–1360, 1120–1070, and 1060–1100 cm^{-1} correspond to C=C olefin structures, C-H aliphatic structures, bending of O-H, C-H hydroxyl, C-O secondary hydroxyl, and the stretching of C-O primary hydroxyl, respectively [29, 30]. The bands at 3664 cm^{-1} attributed to free alcohol. The bands at 1585 and 1469 cm^{-1} are due to primary and secondary amines (N–H) deformations. The C–N stretching of primary and secondary amines also appears at bands of 1076–1177 and 1130 cm^{-1}, respectively. More vibration occurred as can be seen in the bands at 1150–1050 cm^{-1} corresponding to C-O stretching and OH-groups which could justify that the surface of CCAC is ionic and preferable for adsorption of BGD [18]. H_2SO_4 activation also leads to the incorporation of the Sulphur element structure of carbon. Thus, the presence of hydroxyl functional groups is the determinant in facilitating the adsorbent [18]. Generally, as it is observed from Figure 4, the wavelength of the adsorbent decreased after adsorption which indicates that the surface adsorbent is occupied by the BGD, which decreases the transmittance.

X-ray Diffraction (XRD)

It is observed from Figure 5 that the structure of powdered CCAC was predominantly amorphous [31]. The two broad diffractions at 2θ=6.08°, 2θ=23.04°, and less diffraction of 2θ=37.02° correspond to reflections from (299), (712), and (261) before adsorption, and 2θ=5.87 and 23.9°, which correspond to reflections from (2917) and (999) after adsorption. The XRD plots revealed that the diffraction of CCAC slightly decreases after adsorption of BGD [31]. The amorphous content of corncob-activated carbon was due to its structure's high lignin content (amorphous compound). The more amorphous region of activated carbon makes it suitable for more efficient absorbent in separating organic dyes from water and wastewater [32].

Scanning Electron Microscopy (SEM)

The SEM image for both activated carbon samples before adsorption (ACB) and after adsorption (ACA) are shown in Figure 6. It was observed that the activated carbon before adsorption contains holes and pores on its surface than after adsorption which allows for adsorption. The concentration of BGD on the adsorbent's surface may be the cause of the smoother surface shape shown in the SEM pictures of CCAC following adsorption [18]. Based on SEM results, the external surface of both ACB and ACA contains rough pores of different shapes and sizes. The ACB has narrow elongated pores indicating its suitability for adsorption and the large surfaces on ACA show the adsorbent is saturated [18]. It is also evident that based on Figure 6, the surface of CCAC after adsorption of BGD becomes denser and smoother with significant surface morphology.

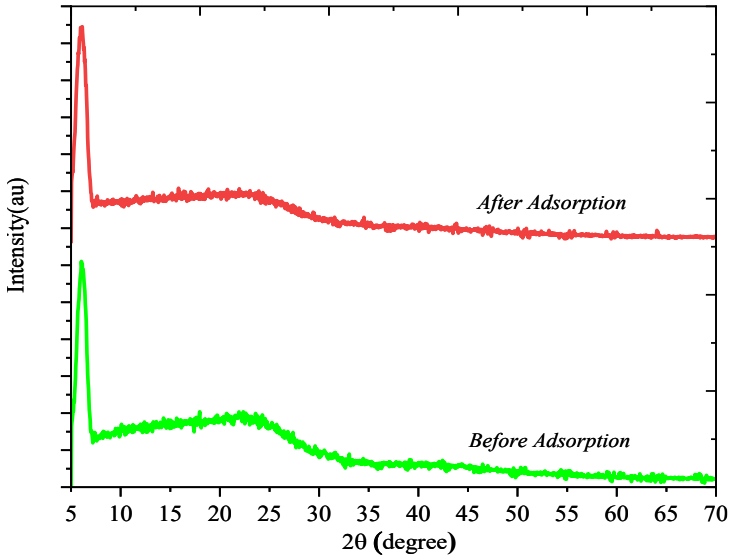

Figure 5. XRD plots of CCAC before and after adsorption.

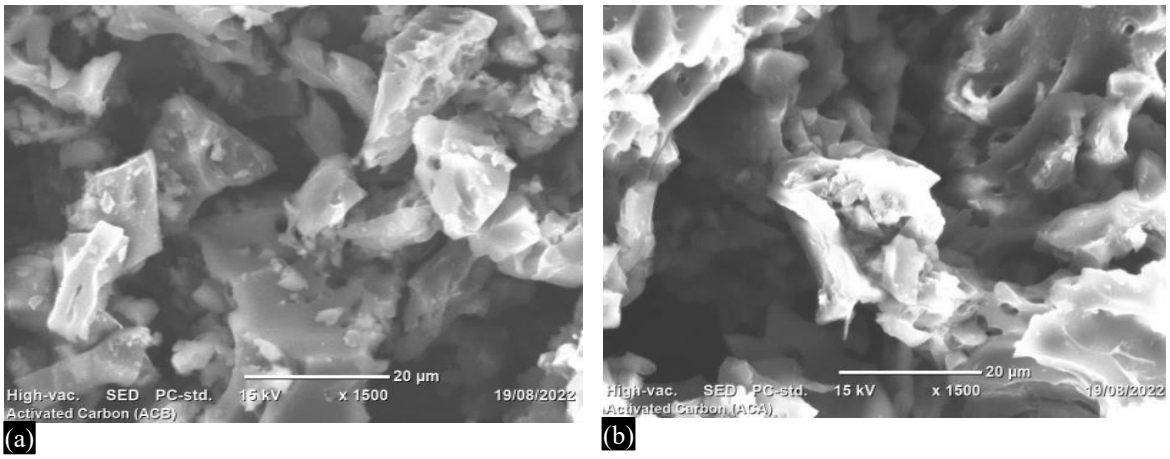

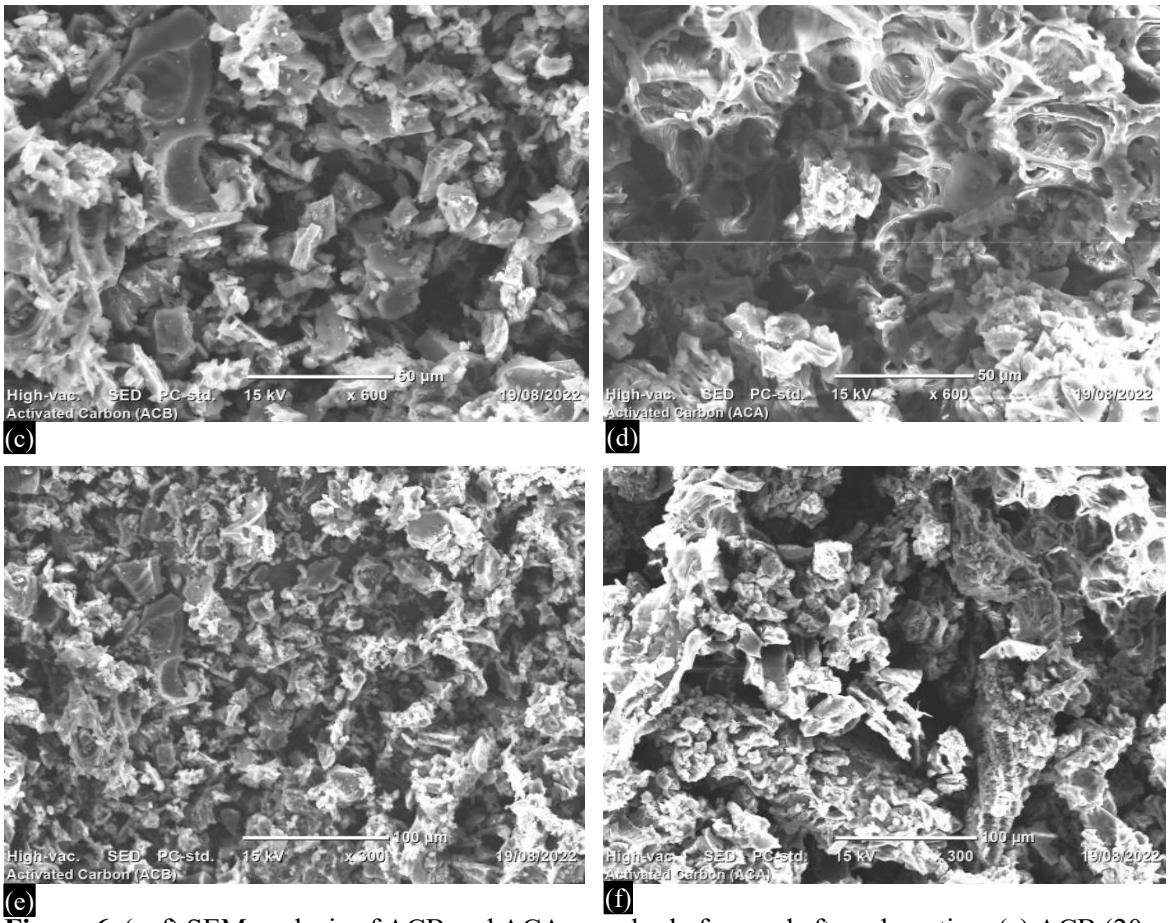

Figure 6. (a–f) SEM analysis of ACB and ACA samples before and after adsorption. (a) ACB (20 µm); (b) ACA (20 µm); (c) ACB (50 µm); (d) ACA (50 µm); (e) ACB (100 µm); (f) ACA (100 µm).

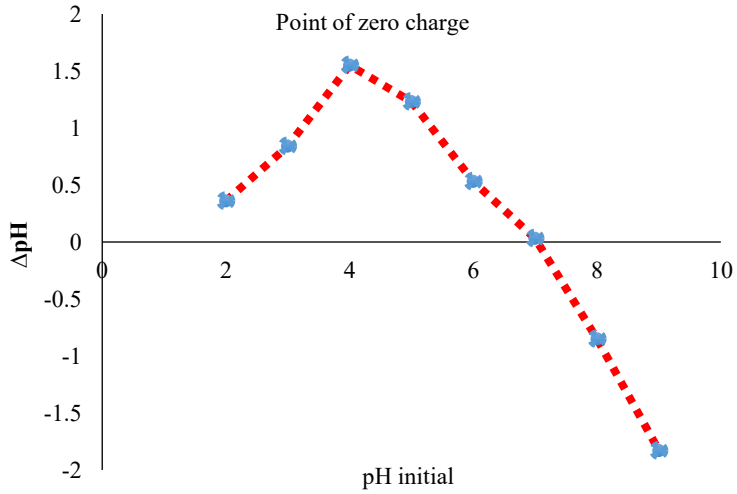

Figure 7. Point of zero charge.

Point of Zero Charge Analysis

The pH of the point of zero charges (pHpzc) of CCAC was calculated by a drift method shown in Figure 7. It was suggested that if pH>pHpzc, the adsorption of cationic dye on adsorbent is suitable, in contrast, if pH<pHpzc the adsorption of anionic species is more favorable. The pH drift is a quick and reliable method for determining the point of zero charges and was suggested to be appropriate for charcoal [33]. In this study, the pHpzc of the CCAC was determined to be around 6.93 which was used

to understand the change in the surface character of the synthesized adsorbent under changing pH values. This illustrates that the CCAC surface has a positive charge when the pH of the solution is below pHpzc and a negative charge when the pH of the solution is higher than pHpzc. A similar finding has been reported by Iheanacho *et al.* [19].

Adsorption Isotherms

The studies of adsorption isotherm were performed by varying initial concentrations of BGD from 10–90 mg/l at room temperature using 100 ml of initial BGD solutions with an adsorbent dose of 0.267 g, shaking speed of 200 rpm, the contact time of 63.85 min and pH of 7.172. The adsorption behavior between the CCAC and BGD ions under different concentrations was interpreted by the Langmuir and Freundlich isotherms models as shown in Figures 8 and 9, respectively. The outcomes are illustrated in Table 1 and it shows the experimental data fit both Langmuir and Freundlich adsorption isotherm models. Based on Figure 9, the adsorbed BDG ions on the surface of CCAC effectively undergo the monolayer and homogeneous adsorption process of BGD ions rather than the multilayer adsorption process [34].

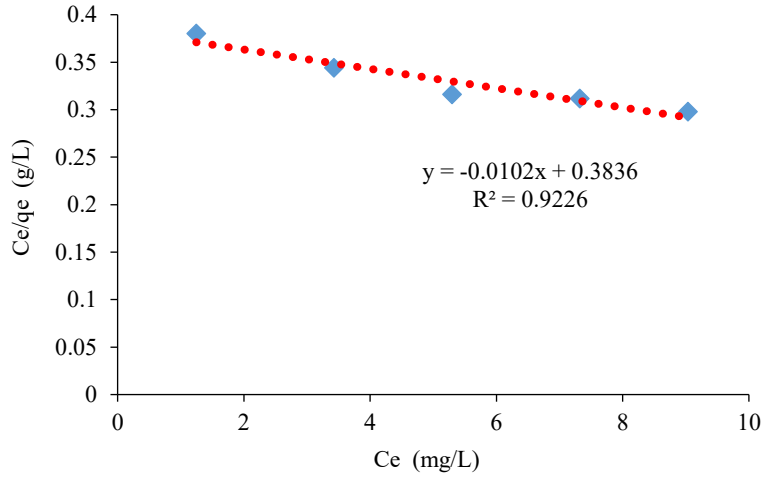

Figure 8. Langmuir isotherm model of BGD removal.

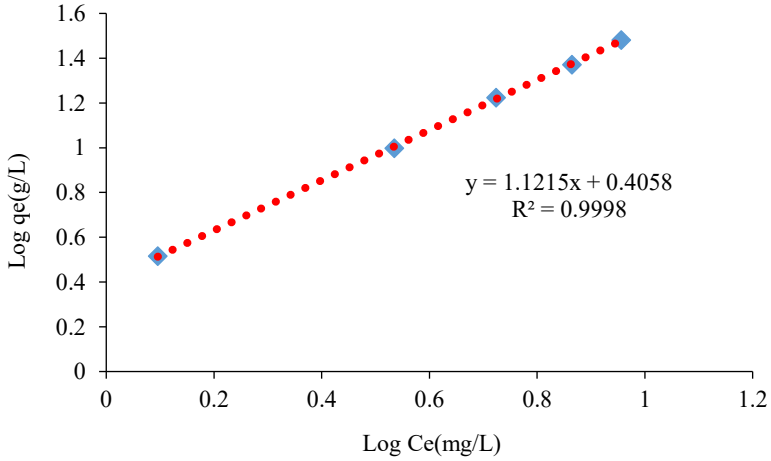

Figure 9. Freundlich isotherm model of BGD removal.

Table 1. Langmuir and Freundlich isotherm models.

	Langmuir			Freundlich			
Adsorbent	***Q_{max} (mg/g)***	***B (mg^{-1})***	***R^2***	***K_f***	***N***	***1/n***	***R^2***
CCAC	98.42	0.026	0.9226	2.54	0.89	1.1215	0.9998

The values of separation factor R_L ($0<R_L<1$) given in Table 2, designate the favorability of the adsorption process with a maximum adsorption capacity (Q_{max}) of 98.04 mg/g (Table 1). Furthermore, a value of the Langmuir coefficient (*b*), which is 0.026 Lm/g implies strong binding sites exist on the surface of the adsorbent indicating the adsorbents could adsorb dyes effectively [35, 36]. On the other hand, as represented in Table 1, the value of the Freundlich constant ($n>1$) shows favorable adsorption [33]. R^2 of 0.999 represents that heterogeneous conditions were existed [37]. This study data revealed that the Freundlich isotherm model fits the experimental data better than the Langmuir isotherm model, with a maximum correlation coefficient that aligns with data reported by Tan *et al*. [38]. The Langmuir separation factor RL is given in Table 2 and Figure 10.

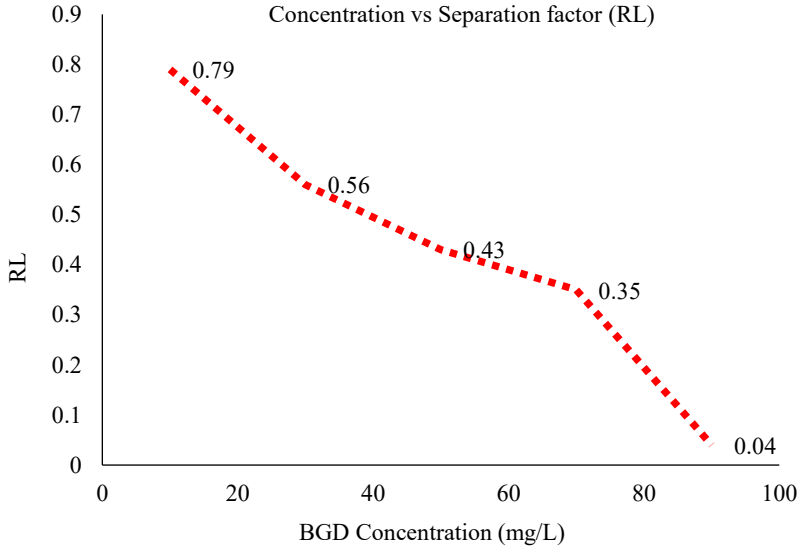

Figure 10. Langmuir separation factor.

Table 2. Langmuir separation factor R_L.

C_o	10	30	50	70	90
R_L	0.79	0.56	0.43	0.35	0.04

Factors Affecting the Adsorption of BDG

Effect of solution pH on BGD removal

The influence of solution pH on BGD removal was tested at room temperature using 100 ml of 40 mg/l; starting BGD solution in the pH range of 2–12, 0.4 g of adsorbent, 200 rpm of shaking, and 40 min of contact time. As demonstrated in Figure 11, the removal of BGD on CCAC is mostly affected by pH solution. At pH 8, the maximum adsorption capacity of 95.7% was reached, after which it declined. The removal of BGD on CCAC increased up to the center point and then decreased. The electrostatic repulsion between the negative charges of the CCAC adsorbent and the cationic species of BGD resulted in significant BGD removal effectiveness at low pH. Increasing the adsorption capacity of CCAC with increasing pH indicates that negative charge increases on the surface of the adsorbent, which causes the deprotonation of functional groups available in CCAC which act as sites for the binding of cationic BGD [39]. The low adsorption capacity at very low pH may be due to the competition of protons with dye molecules available at the active sites of adsorbent [40]. According to the study conducted by Mansour *et al.* [41], increasing the pH from 1 to 10 has enhanced the dye removal percentage from 55.94 to 90.93%. The maximum adsorption capacity was 9.57 mg/g at a pH of 8. This demonstrates that the pH of the solution has a significant impact on the BGD adsorption process.

Effect of Contact Time

The most important factor influencing the adsorption process is contact time [42]. To determine the time for attainment of equilibrium, batch studies were performed at room temperature for 20–100 min,

with 10 min intervals using 100 ml of 40 mg/l initial BGD solutions at an adsorbent dosage of CCAC of 0.3 g, a shaking speed of 200 rpm, and a pH of 8. The experimental results for the effect of contact time are shown in Figure 12. It was perceived that around 94.37% of BGD was removed during the first 20 min of adsorption, indicating that the adsorption of BGD onto CCAC was fast during the beginning stage of the adsorption process. The presence of a large number of free negatively charged active sites on the adsorbent surface resulted in the rapid removal of BGD. On the other hand, lengthening the contact time after 60 min did not show a significant influence on BGD adsorption. Generally, during the first minutes of adsorption, the number of active sites on the adsorbent surface is much greater than the remaining sites. In the case of high contact times, the molecules need more time to diffuse inside the pore of the adsorbent. Therefore, the adsorption was maximum in the first stages of the adsorption process [37].

Effect of CCAC Dosage

At room temperature, the effect of the adsorbent dose on the removal of cationic BGD from an aqueous solution was examined by varying the adsorbent dose (0.1, 0.2, 0.3, 0.4, and 0.5 g) with an initial BGD concentration of 40 mg/l. Firstly, the solutions were shaken for 40 min at 200 rpm at a pH of 8. The residuals of BGD ions were studied after each sample was filtered with the Whatman №40 filter paper.

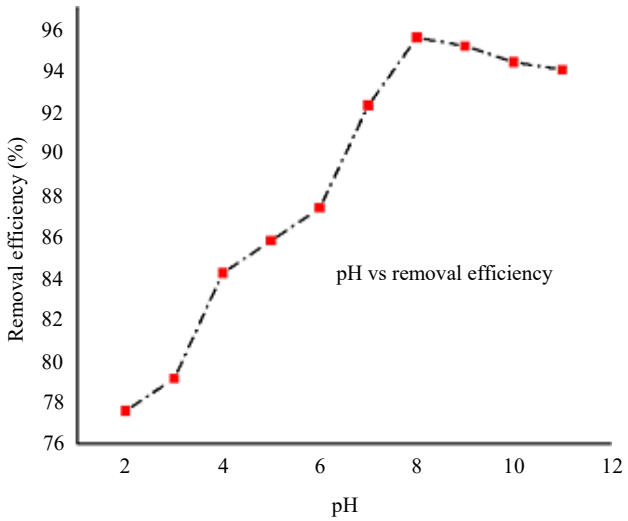

Figure 11. Effect of PH on BGD removal efficiency.

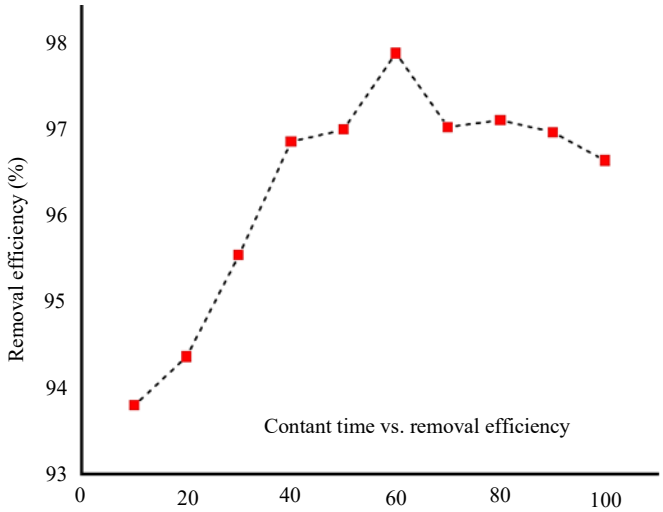

Figure 12. Effect of contact time on BGD adsorption.

The effect of the adsorbent dose was particularly studied as important for the removal of BGD, and the results obtained are shown in Figure 13. The findings show that as the dose of CCAC was increased from 0.1 to 0.3 g the percentage removal of BGD increased from 93.2 to 98.1%. Increasing the adsorption capacity was limited when it achieved the saturation point. However, the aggregation of adsorbent particles at higher dosages leads to a decrease in the surface area which reduces the adsorption effectiveness of the adsorbate [43]. The higher the dosage, the lower the adsorption capacity. At 0.1 g, the highest adsorption capacity (Q_{max}) was 37.4 mg/g. Similar findings were reported by Al-Jaafari and Al-Kazragi [44].

The Effect of Initial Concentrations

At room temperature, the effect of initial BGD concentration on the removal of BGD ions from aqueous solution by CCAC was studied by varying the initial concentration from 10 to 90 mg/l with intervals of 10 mg/l while other parameters such as the adsorbent dose, contact time and pH were maintained constant at values of 0.3 g, 60 min, and 8, respectively. The solutions were stirred for 60 min at 200 rpm, and then each sample was filtered through Whatman №40 filter paper before being tested for BGD solutions following the procedures given by Abbas [45]. The results obtained for the effects of initial BGD concentration on BGD removal are shown in Figure 14.

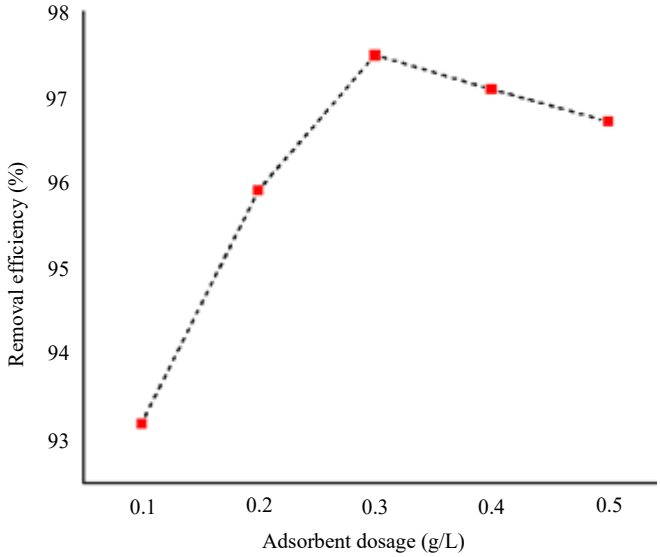

Figure 13. Effect of adsorbent dosage on BGD removal.

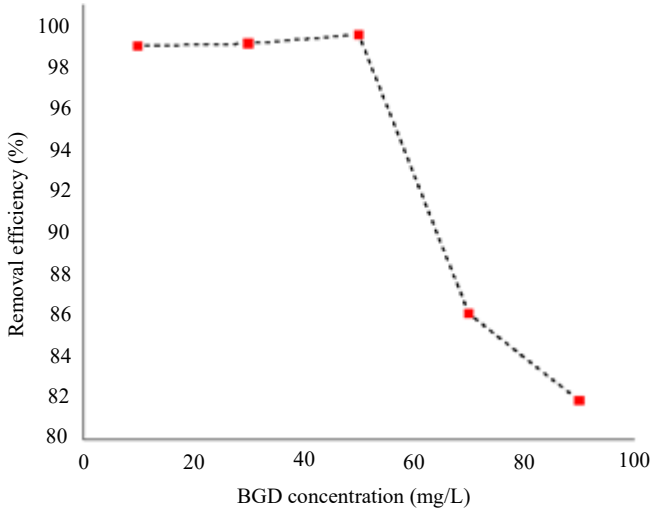

Figure 14. Effect of initial BGD for removal efficiency of BGD.

It was noticed that increasing the initial concentration of BGD resulted in a lower percentage elimination of BGD. In this study, the removal efficiency of 99.56% was obtained at a minimum value of BGD concentration and 81.87% was obtained at a maximum concentration of BGD. Therefore, most of the dye molecules are adsorbed by adsorbents at low initial dye concentrations and the removal efficiencies increase. A study reported that when an initial dye concentration is in excess, the active sites of the adsorbent are completely retained, so some of the dye molecules cannot be absorbed, and the removal efficiencies decrease [46].

Factors Affecting Desorption of BDG

Effect of Initial Concentrations on Desorption of BGD

The effect of initial dye concentrations was studied at concentrations of 10, 30, 50, 70, and 90 mg/l of BGD, and the maximum desorption efficiency was obtained at 50 mg/l. Adsorbent dosage, pH, contact time, and agitation speed were all maintained at 8, 60 min, 0.26 g, and 200 rpm, respectively. The maximum desorption efficiency was 91.8% for the first cycle and the minimum value was obtained as 67% for the second cycle as shown in Figure 15.

Effect of Eluents Concentrations

In this study, the effect of three different concentrations of eluents: HCl, NaCl, and CH_3OH with concentrations of 0.125, 0.25, 0.5, and 1 M was examined in BGD desorption efficiency. The results obtained are revealed in Figure 16. Based on the obtained data, increase in the concentration of eluents increases the desorption efficiency. Study findings shows that the highest and lowest desorption efficiency was obtained at 90% at 1 M HCl, and 43.5% at 0.125 M CH_3OH.

Effect of HCl:CH_3OH Ratios

The effect of HCl:CH_3OH ratios was examined at HCl: CH_3OH ratios of 1:0, 3:1, 1:3, and 0:1. As shown in Figure 17, the highest and lowest desorption efficiency was obtained at 1:0 of HCl in first cycle and 0:1 M of CH_3OH in second cycle which indicates the acid was more effective than alcohol for the desorption of CCAC. This implies that higher molecular alcohols have less desorption efficiency than lower molecular alcohols [9].

The comparison of different adsorbents for BGD removal is shown in Table 3.

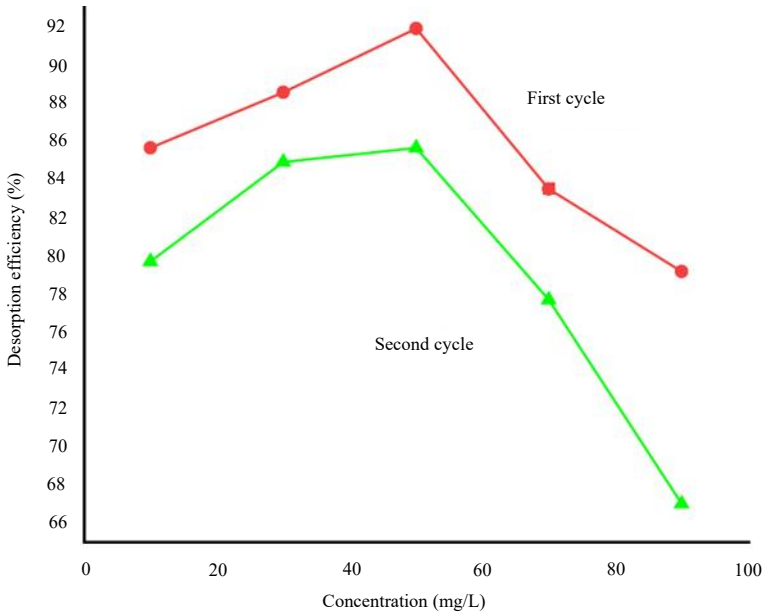

Figure 15. Effect of initial concentration in desorption of BG.

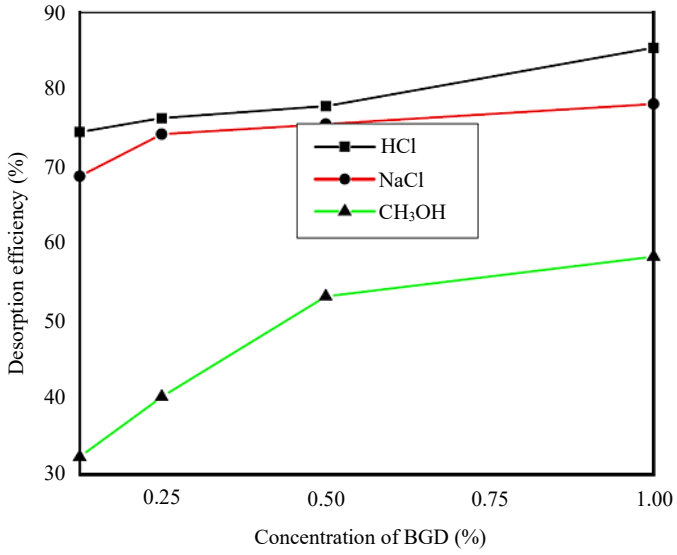

Figure 16. Effect of eluents concentrations.

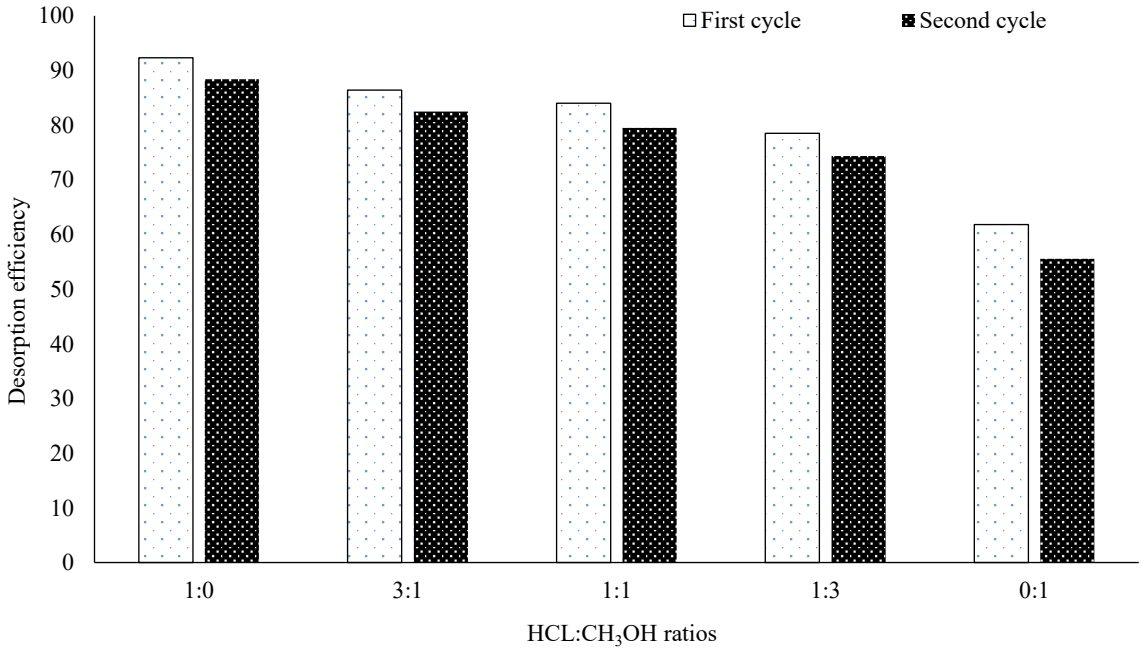

Figure 17. Effect of HCl:CH_3OH ratios in desorption of BGD.

Table 3. Comparison of different adsorbents for BGD removal.

Adsorbent	Co (mg/l)	Adsorption Capacity (mg/g)	Removal efficiency (%)	References
Pyrus pashia leaves	10		93.35	[47]
Activated carbon from guava seeds	10	80.5	98	[48]
Fava bean peels (FBP)	5	28.14	84	[49]
Lawsonia inermis seed powder	20	34.96	93%	[50]
Corn cobs activated carbon	59.463	98.04	99.31	This study findings

CONCLUSION

In this study, corncob-activated carbon (CCAC) adsorbents were prepared using the H_2SO_4 activation method for the removal of brilliant green dye (BGD) from synthetic wastewater. The produced CCAC

was characterized by performing XRD, SEM, and FTIR spectroscopy. The XRD data showed that the CCAC samples are amorphous substances. The FTIR spectrum showed that the CCAC's chemical structure included a variety of functional groups. The morphology of CCAC was studied from the SEM image analysis. The parameters influencing the synthesized CCAC's adsorption and desorption efficiency were examined in this work. As a result, the maximum adsorption efficiency of 95.7, 94.37, 98.1, and 99.56% at pH=8, contact time =20 min, the dosage of CCAC=0.3 g, and initial concentration =43 mg/l, respectively. Besides, the BGD removal fits more into the Freundlich isotherm model than the Langmuir model with a correlation coefficient R^2 of 0.999. In addition, the effects of eluent concentration, BGD concentrations, and acid: alcohol ratio on the desorption of BGD were conducted. Maximum desorption efficiency was obtained at 1 M HCl. The adsorption capacity of prepared CCAC was 98.04 mg/g. In general, this study showed that CCAC was an efficient biomass adsorbent for the removal of BDG that can be easily prepared and regenerated at low cost.

Conflicts of Interest

Authors declare no conflict of interest.

Funding

No funding was received for this research work.

Data Availability Statement

The raw datasets used and/or analyzed during the present work are available from the corresponding author at reasonable request at any time.

REFERENCES

1. Chowdhury M, Mostafa MG, Biswas TK, Mandal A, Saha AK. Characterization of the effluents from leather processing industries. Environ Process. 2015 Mar; 2: 173–87.
2. Saravanan A, Kumar PS, Jeevanantham S, Karishma S, Tajsabreen B, Yaashikaa PR, Reshma B. Effective water/wastewater treatment methodologies for toxic pollutants removal: Processes and applications towards sustainable development. Chemosphere. 2021 Oct 1; 280: 130595.
3. Gürses A, Açıkyıldız M, Güneş K, Gürses MS. Dyes and pigments: Their structure and properties. In: Dyes and Pigments. SpringerBriefs in Molecular Science. Cham: Springer; 2016. doi: 10.1007/978-3-319-33892-7_2.
4. Hintz NH, *et al*. Ecological impacts of photosynthetic light harvesting in changing aquatic environments: A systematic literature map. Ecol Evol. 2022; 12(3): e8753.
5. Vigneshpriya D, Krishnaveni N, Renganathan S, Sri Sakthi Priyadarshini R. Impact of untreated and Sargassum wightii-treated brilliant green dye exposure on Indian major carp, Labeo rohita Ham.: hematology, biochemistry, enzymology and histopathology. Int J Phytoremediation. 2020 Jul 2; 22(8): 819–26.
6. Zhang L, Sellaoui L, Franco D, Dotto GL, Bajahzar A, Belmabrouk H, Bonilla-Petriciolet A, Oliveira ML, Li Z. Adsorption of dyes brilliant blue, sunset yellow and tartrazine from aqueous solution on chitosan: Analytical interpretation via multilayer statistical physics model. Chem Eng J. 2020 Feb 15; 382: 122952.
7. Sabir A, Altaf F, Batool R, Shafiq M, Khan RU, Jacob KI. Agricultural waste absorbents for heavy metal removal. Green adsorbents to remove metals, dyes and boron from polluted water. Cham: Springer; 2021; 195–228.
8. Rahma NA, Kurniasari A, Pambudi YD, Bintang HM, Zulfia A, Hudaya C. Characteristics of corncob-originated activated carbon using two different chemical agent. In IOP Conf Ser: Mater Sci Eng (IOP Publishing). 2019 Oct 1; 622(1): 012030.
9. Kumaravel S, Geetha M, Niyitanga T, Kumar DS, Al-Ansari MM, Mythili R, Suganthi S, Guganathan L, Murugan A, Ragupathy S. Preparation and characterization of activated carbon from corn cob by chemical activation and their adsorption of brilliant green dye from wastewater. Process Saf Environ Prot. 2024 Aug 1; 188: 1338–45.

10. Berber-Villamar NK, Netzahuatl-Muñoz AR, Morales-Barrera L, Chávez-Camarillo GM, Flores-Ortiz CM, Cristiani-Urbina E. Corncob as an effective, eco-friendly, and economic biosorbent for removing the azo dye Direct Yellow 27 from aqueous solutions. PLoS One. 2018 Apr 26; 13(4): e0196428.
11. Aljeboree AM, Hussein FH, Alkaim AF. Removal of textile dye (methylene blue mb) from aqueous solution by activated carbon as a model (corn-cob source waste of plant): As a model of environmental enhancement. Plant Arch. 2019; 19(2): 906–9.
12. Değermenci GD, Değermenci N, Ayvaoğlu V, Durmaz E, Çakır D, Akan E. Adsorption of reactive dyes on lignocellulosic waste; characterization, equilibrium, kinetic and thermodynamic studies. J Clean Prod. 2019 Jul 10; 225: 1220–9.
13. Akperov EO, Akperov OH. The wastage of the cotton stalks (Gossypium hirsutum L.) as low-cost adsorbent for removal of the Basic Green 5 dye from aqueous solutions. Appl Water Sci. 2019 Nov; 9(8): 183.
14. Kallel F, Chaari F, Bouaziz F, Bettaieb F, Ghorbel R, Chaabouni SE. Sorption and desorption characteristics for the removal of a toxic dye, methylene blue from aqueous solution by a low cost agricultural by-product. J Mol Liq. 2016 Jul 1; 219: 279–88.
15. Meskel AG, Kwikima MM, Meshesha BT, Habtu NG, Naik SC, Vellanki BP. Malachite green and methylene blue dye removal using modified bagasse fly ash: Adsorption optimization studies. Environ Chall. 2024 Jan 1; 14: 100829.
16. Song M, Jin B, Xiao R, Yang L, Wu Y, Zhong Z, Huang Y. The comparison of two activation techniques to prepare activated carbon from corn cob. Biomass Bioenergy. 2013 Jan 1; 48: 250–6.
17. Kolur NA, Sharifian S, Kaghazchi T. Investigation of sulfuric acid-treated activated carbon properties. Turk J Chem. 2019; 43(2): 663–75.
18. Wibawa PJ, Nur M, Asy'ari M, Nur H. SEM, XRD and FTIR analyses of both ultrasonic and heat generated activated carbon black microstructures. Heliyon. 2020 Mar 1; 6(3): e03546.
19. Iheanacho OC, Nwabanne JT, Obi CC, Igwegbe CA, Onu CE, Dahlan I. Adsorptive dephenolization of aqueous solutions using thermally modified corn cob: mechanisms, point of zero charge, and isosteric heat studies. Adsorpt Sci Technol. 2023 Apr 13; 2023: 2813663.
20. Ali AF, Kovo AS, Adetunji SA. Methylene blue and brilliant green dyes removal from aqueous solution using agricultural wastes activated carbon. J Encapsul Adsorpt Sci. 2017 Jun 12; 7(2): 95–107.
21. Mansour RA, Simeda MG, Zaatout AA. Removal of brilliant green dye from synthetic wastewater under batch mode using chemically activated date pit carbon. RSC Adv. 2021; 11(14): 7851–61.
22. Aldabib J, Edbeib M. The effects of concentration based on the absorbance form the ultraviolet–visible (UV-VIS) spectroscopy analysis. International Journal of Science Letters (IJSL). 2020; 2(1): 1–11.
23. Laskar N, Kumar U. Removal of Brilliant Green dye from water by modified Bambusa Tulda: adsorption isotherm, kinetics and thermodynamics study. Int J Environ Sci Technol. 2019 Mar 14; 16: 1649–62.
24. Vithalkar S, Jugade RM, Saravanan D. Adsorption of brilliant green dye by used-tea-powder: Equilibrium, kinetics and thermodynamics studies. AQUA—Water Infrastruct Ecosyst Soc. 2022 Oct 1; 71(10): 1148–58.
25. Wibowo E, Rokhmat M, Abdullah M. Reduction of seawater salinity by natural zeolite (Clinoptilolite): Adsorption isotherms, thermodynamics and kinetics. Desalination. 2017 May 1; 409: 146–56.
26. Idan IJ, Abdullah LC, Choong TS, Jamil SN. Equilibrium, kinetics and thermodynamic adsorption studies of acid dyes on adsorbent developed from kenaf core fiber. Adsorpt Sci Technol. 2018 Feb; 36(1–2): 694–712.
27. Okeola FO, Odebunmi EO. Freundlich and langmuir isotherms parameters for adsorption of methylene blue by activated carbon derived from agrowastes. Adv in Nat Appl Sci. 2010 Sep 1; 4(3): 281–9.

28. Zanella O, Tessaro IC, Féris LA. Desorption-and decomposition-based techniques for the regeneration of activated carbon. Chem Eng Technol. 2014 Sep; 37(9): 1447–59.
29. IkhtiarBakti A, Gareso PL. Characterization of active carbon prepared from coconuts shells using FTIR, XRD and SEM techniques. J Ilm Pendidik Fis Al-Biruni. 2018; 7(1): 33–9.
30. Dittmann D, Saal L, Zietzschmann F, Mai M, Altmann K, Al-Sabbagh D, Schumann P, Ruhl AS, Jekel M, Braun U. Characterization of activated carbons for water treatment using TGA-FTIR for analysis of oxygen-containing functional groups. Appl Water Sci. 2022 Aug; 12(8): 203.
31. Kunusa WR, Iyabu H, Abdullah R. FTIR, SEM and XRD analysis of activated carbon from sago wastes using acid modification. In J Phys: Conf Ser (IOP Publishing). 2021 Jul 1; 1968(1): 012014.
32. Lee SM, Lee SH, Roh JS. Analysis of activation process of carbon black based on structural parameters obtained by XRD analysis. Crystals. 2021 Feb 2; 11(2): 153.
33. Mane VS, Mall ID, Srivastava VC. Kinetic and equilibrium isotherm studies for the adsorptive removal of Brilliant Green dye from aqueous solution by rice husk ash. J Environ Manag. 2007 Sep 1; 84(4): 390–400.
34. Gürses A, Yalvac D, Güneş K, Şahin E, Açıkyıldız M. The adsorption–desorption mechanisms on the powdered activated carbon (PAC) of an anionic textile dye (RBY 3GL). Desalin Water Treat. 2017 Apr 1; 70: 134–8.
35. Kong L, Qiu F, Zhao Z, Zhang X, Zhang T, Pan J, Yang D. Removal of brilliant green from aqueous solutions based on polyurethane foam adsorbent modified with coal. J Clean Prod. 2016 Nov 20; 137: 51–9.
36. Kołodyńska D, Krukowska JA, Thomas P. Comparison of sorption and desorption studies of heavy metal ions from biochar and commercial active carbon. Chem Eng J. 2017 Jan 1; 307: 353–63.
37. Samiyammal P, Kokila A, Pragasan LA, Rajagopal R, Sathya R, Ragupathy S, Krishnakumar M, Reddy VR. Adsorption of brilliant green dye onto activated carbon prepared from cashew nut shell by KOH activation: Studies on equilibrium isotherm. Environ Res. 2022 Sep 1; 212: 113497.
38. Tan IA, Ahmad AL, Hameed BH. Adsorption isotherms, kinetics, thermodynamics and desorption studies of 2, 4, 6-trichlorophenol on oil palm empty fruit bunch-based activated carbon. J Hazard Mater. 2009 May 30; 164(2–3): 473–82.
39. Calvete T, Lima EC, Cardoso NF, Dias SL, Ribeiro ES. Removal of brilliant green dye from aqueous solutions using home made activated carbons. Clean–Soil, Air, Water. 2010 Jun; 38(5–6): 521–32.
40. Mansour RA, El Shahawy A, Attia A, Beheary MS. Brilliant green dye biosorption using activated carbon derived from guava tree wood. Int J Chem Eng. 2020; 2020(1): 8053828.
41. Mansour RA, Simeda MG, Zaatout AA. Removal of brilliant green dye from synthetic wastewater under batch mode using chemically activated date pit carbon. RSC Adv. 2021; 11(14): 7851–61.
42. Singh S, Gupta H, Dhiman S, Sahu NK. Decontamination of cationic dye brilliant green from the aqueous media. Appl Water Sci. 2022 Apr; 12(4): 61.
43. Silva TL, Ronix A, Pezoti O, Souza LS, Leandro PK, Bedin KC, Beltrame KK, Cazetta AL, Almeida VC. Mesoporous activated carbon from industrial laundry sewage sludge: Adsorption studies of reactive dye Remazol Brilliant Blue R. Chem Eng J. 2016 Nov 1; 303: 467–76.
44. Al-Jaafari AK, Al-Kazragi MA. Efficient Removal of Brilliant Green Dye Using Mesoporous Attapulgite Clay: Investigating Adsorption Kinetics, Isotherms, and Mechanisms. Sci World J. 2024; 2024(1): 9799127.
45. Abbas M. Removal of brilliant green (BG) by activated carbon derived from medlar nucleus (ACMN)–Kinetic, isotherms and thermodynamic aspects of adsorption. Adsorpt Sci Technol. 2020 Dec; 38(9–10): 464–82.
46. Amjah AN, Abdulhameed AS, Jawad AH, ALOthman ZA, Wilson LD. Activated carbon from noodles food waste via microwave-assisted KOH for optimized brilliant green dye removal. Biomass Convers Biorefinery. 2024 Dec; 14(23): 30355–67.
47. Hama Aziz KH, Fatah NM, Muhammad KT. Advancements in application of modified biochar as a green and low-cost adsorbent for wastewater remediation from organic dyes. R Soc Open Sci. 2024 May 15; 11(5): 232033.

48. Al-Hazmi GA, Alayyafi AA, El-Desouky MG, El-Bindary AA. Guava seed activated carbon loaded calcium alginate aerogel for the adsorption of diclofenac sodium: characterization, isotherm, kinetics, and optimization via Box-Behnken design. Int J Biol Macromol. 2024 Mar 1; 262: 129995.
49. Husien S, El-taweel RM, Alrefaey K, Labena A, Fahim IS, Said LA, Radwan AG. Experimental investigation of methyl-orange removal using eco-friendly cost-effective materials raw fava bean peels and their formulated physical, and chemically activated carbon. Curr Res Green Sustain Chem. 2023 Jan 1; 7: 100373.
50. Khammee P, Unpaprom Y, Whangchai K, Ramaraj R. Comparative studies of the longan leaf pigment extraction as a photosensitizer for dye-sensitized solar cells' purpose. Biomass Convers Biorefinery. 2022 May; 12(5): 1619–26.

